A Novel Ventricular Digital Twin: Modeling Transmural Scar Heterogeneity and Purkinje–Myocardial Junction

Fuyu Cheng[1], Johanna Tonko[2], Elisa Rauseo[1], Semhar B Misghina[1], Carlos E Barrera[1], Edward J Vigmond[3], Gregory Slabaugh[1], Nay Aung[1], Pier Lambiase[2], Steffen E Petersen[1], Caroline H Roney[1]

[1] Queen Mary University of London, United Kingdom [2] Institute of Cardiovascular Science, University College London, United Kingdom [3] University of Bordeaux, France

Abstract

Biventricular digital twins (BDTs) offer personalized simulations of cardiac electrophysiology but often omit key determinants of conduction, such as transmural scar heterogeneity and Purkinje–myocardial junctions (PMJs). We developed a pipeline integrating LGE-CMR–based transmural scar modelling with anatomically informed PMJ deployment. Clinical local activation time (LAT) maps were used for patient-specific calibration, and simulations were performed in three ventricular tachycardia (VT) patients. The models achieved sub-10 ms LAT accuracy (mean error 6.11 ± 3.26 ms, RMSE 6.85 ms) and reproduced clinically consistent reentry locations. Incorporating PMJ and scar details improved activation realism and arrhythmia reproducibility, demonstrating a step toward non-invasive VT risk assessment and individualized ablation planning.

1. Introduction

Biventricular digital twins (BDTs) enable patient-specific simulations of cardiac function, arrhythmia risk, and treatment response by integrating anatomical, imaging, and electrophysiological data [1]. Despite recent progress, most BDTs incompletely represent the interplay between structural remodeling and conduction system physiology, omitting key determinants of arrhythmogenesis.

Many ventricular models adopt simplified scar descriptions, treating scar as a two-dimensional surface or homogeneous inexcitable volume, neglecting transmural heterogeneity essential for slow-conduction channels and reentrant circuits[2]. Moreover, the Purkinje network and its Purkinje–myocardial junctions (PMJs), crucial for coordinated ventricular activation, are often excluded, leading to systematic activation-time errors [3].

We present a pipeline integrating (i) transmural scar modelling from late gadolinium enhancement (LGE) cardiac magnetic resonance (CMR) and (ii) anatomically informed PMJ deployment. Local activation time (LAT) – based calibration refined conduction parameters, and models were evaluated through ventricular tachycardia (VT) induction and reentry simulations.

2. Methods

2.1. Data Acquisition & Mesh Generation

Three patients with ischemic cardiomyopathy–related VT who underwent LGE-CMR, electrogram (EGM) mapping, and ECG were selected.

The workflow for CMR-based reconstruction and analysis is shown in Figure 1. Nine LV and one RV meshes containing scar annotations were generated using ADAS 3D [4], and combined into a 0.4 mm tetrahedral biventricular mesh, consistent with recommended monodomain simulation resolution [5, 6]. Myocardial fiber orientation was assigned using the Laplace–Dirichlet Rule-Based (LDRB) algorithm [7].

2.2. Transmural Scar & Fibrosis Modelling

LGE-CMR signal intensities were thresholded to define: dense fibrosis (DF, $\geqslant$ 60% MPI), border zone (BZ, 40–60% MPI), and healthy tissue (HT, $\leqslant$ 40% MPI) [4, 8]. Scar information from the LV and RV meshes was mapped to the volumetric model using a custom Python-based point-to-point algorithm with distance-weighted interpolation, ensuring faithful transmural distribution.

2.3. PMJ Generation & Conductivity Tuning

A sub-endocardial layer (10% LV wall thickness) was extracted to host PMJs, reflecting anatomical evidence that PMJs penetrate 1–2 mm beneath the endocardium (LV wall: 8–12 mm) [9]. Recent myosin light chain 4 (MYL4) immunolabeling studies further demonstrated that over 60% of Purkinje fibers form an intramural network intercalating within the myocardium,

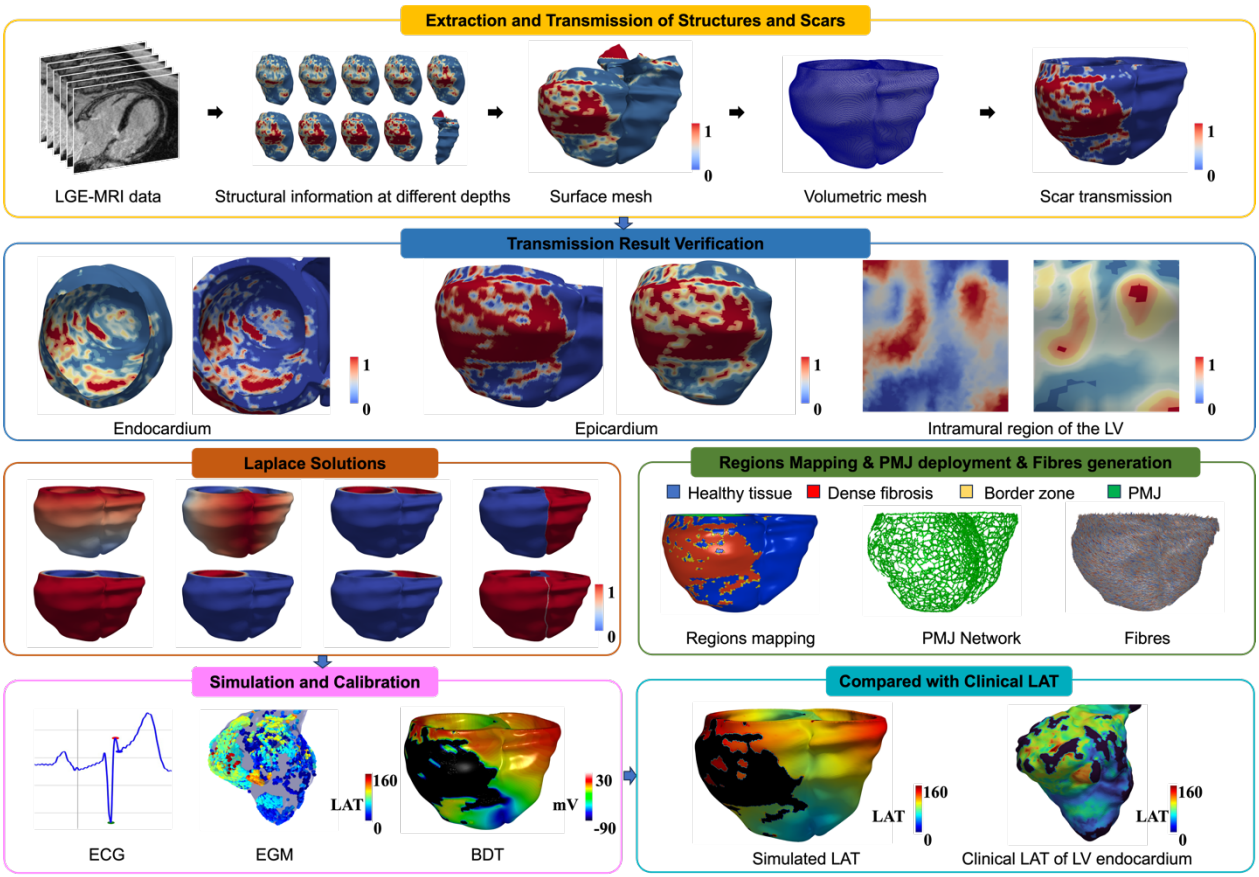

Figure 1. Overview of the BDT construction pipeline

challenging the conventional view of an exclusively subendocardial system [10].

A MATLAB-based algorithm distributed PMJ nodes within this layer, preserving distal reconnection while reducing PMJ density within BZ regions, consistent with fibrosis-induced conduction disruption [11].

PMJ conductivity was tuned using clinical LAT maps. The pacing site served as the primary calibration reference, with a secondary basal LV site along a scar-free pathway. Conductivity was iteratively adjusted until simulated LATs matched clinical data at both sites.

2.4. Electrophysiological Modelling

Simulations were conducted in CARPentry. HT used the Ten Tusscher–Panfilov 2006 (TT2) model; BZ applied TT2 with reduced ionic conductances, INa 38%, ICaL 31%, IKr 30%, IKs 20% of control [12]. DF was non-conductive. Purkinje cells followed the validated Trovato model [13]. HT longitudinal and transverse conductivities were derived from ECG-based velocity estimates. In BZ region, transverse conductivity was reduced 90% to represent Cx43 remodeling [14], longitudinal values remained unchanged.

2.5. Validation & VT Induction

Simulated LATs were compared with clinical LATs at 10 representative endocardial points per patient. Mean absolute error quantified model accuracy. VT inducibility was tested via S1–S2 pacing.

Reentry was defined as sustained >3 cycles with closed-loop propagation. Simulated circuits were compared with clinical ablation sites for spatial agreement.

3. Results

3.1. LAT Accuracy

Simulated LATs matched clinical LATs at 10 representative validation points from the BDT of Patient A (Table 1). Mean absolute LAT error was 6.11 ± 3.26 ms (RMSE = 6.85 ms), with no bias toward early or delayed activation and a maximum deviation of 11.55 ms. The integrated PMJ calibration and transmural scar modelling produced physiologically consistent conduction dynamics across heterogeneous regions.

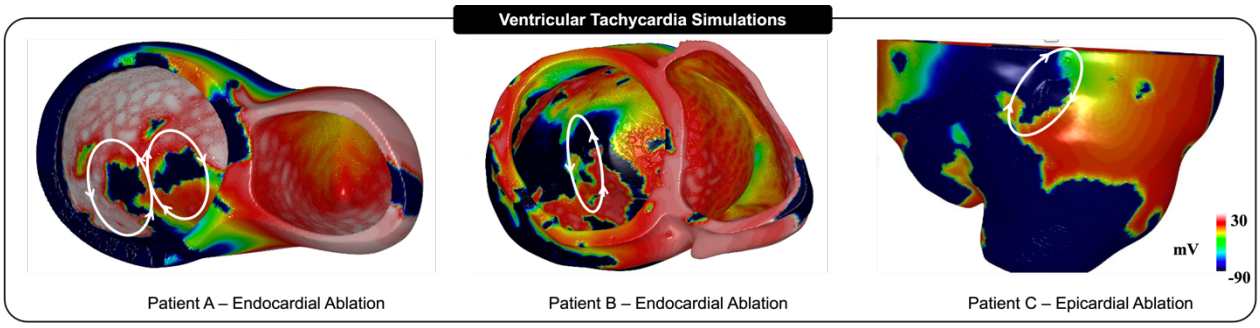

Figure 2. Patient-specific VT induction and reentry circuit simulations

3.2. VT Induction & Reentry Circuits

Sustained VT was inducible in all three patient-specific models (Figure 2). In Patients A and B, reentry arose only via endocardial pacing, localizing to peri-scar slow-conduction channels; reentrant isthmuses overlapped with clinical ablation sites. In Patient C, VT occurred exclusively from epicardial pacing, with activation traversing epicardial BZ regions consistent with ablation targets.

Across all models, endocardial/epicardial inducibility and reentry topology mirrored clinical observations, validating both electrophysiological calibration and anatomical fidelity of the framework.

4. Discussion

4.1. Key Contributions

This study addresses two major BDT limitations: oversimplified scar representation and omission of Purkinje conduction, achieving accurate LAT and VT circuit reproduction. Integrating PMJ deployment with transmural scar modelling enhances physiological realism and predictive capacity.

4.2. Comparison with Prior Work

Camps et al. [3] incorporated realistic Purkinje networks without scar detail. Villar-Valero et al. [15] analysed BZ geometry without Purkinje fibers. Our framework unites these, bridging anatomy and electrophysiology. Recent reviews highlight that accurate representation of scar and conduction systems is essential for advancing non-invasive VT risk assessment [16]; our findings demonstrate a feasible implementation.

4.3. Limitations & Future Directions

Point	Clinical LAT (ms)	Simulated LAT (ms)	Difference (Sim – Clin, ms)
1	27.5	29.44	−1.94
2	31.91	36.44	−4.53
3	49.88	58.56	−8.67
4	121.71	129.75	−8.04
5	85.39	73.84	11.55
6	89.54	94.47	−4.93
7	25.24	27.04	−1.79
8	52.02	59.08	−7.06
9	84.99	94.01	−9.02
10	58.95	55.35	3.6
Mean ± SD	–	–	6.11 ± 3.26 ms
RMSE	–	–	6.85 ms

Table 1. Comparison of simulated and clinical LATs at ten representative endocardial sites from Patient A. Mean absolute error = 6.11 ± 3.26 ms (RMSE = 6.85 ms); all deviations < 12 ms.

PMJ deployment was anatomy-based rather than patient-imaged, and calibration relied on two reference sites, limiting parameter uniqueness. Future work will explore probabilistic inference of Purkinje networks from ECG [17] and machine learning–based optimisation to enable clinically feasible real-time modelling and personalised ablation planning.

5. Conclusion

We developed a physiologically detailed pipeline for constructing biventricular digital twins integrating transmural scar and anatomically guided PMJ deployment. In three VT patients, the models achieved sub-10 ms LAT accuracy and reproduced clinically observed reentry locations. This framework advances non-invasive VT risk stratification and individualised ablation planning with strong translational potential for precision electrophysiology.

References

[1] Corral-Acero, J., et al., The 'digital twin' to enable the vision of precision cardiology. European Heart Journal, 2020. 41(48): p. 4556-4564.

[2] Cedilnik, N., et al., Efficient patient-specific simulations of ventricular tachycardia based on computed tomography-defined wall thickness heterogeneity. JACC: Clinical Electrophysiology, 2023. 9(12): p. 2507-2519.

[3] Camps, J., et al., Digital twinning of the human ventricular activation sequence to clinical 12-lead ecgs and magnetic resonance imaging using realistic purkinje networks for in silico clinical trials. Medical Image Analysis, 2024. 94: p. 103108.

[4] De Silva, K., et al., Whole-heart histological and electroanatomic assessment of postinfarction cardiac magnetic resonance imaging scar and conducting channels. Circulation: Arrhythmia and Electrophysiology, 2024. 17(9): p. e012922.

[5] Neic, A., et al., Efficient computation of electrograms and ecgs in human whole heart simulations using a reaction-eikonal model. Journal of Computational Physics, 2017. 346: p. 191-211.

[6] Prakosa, A., et al., Personalized virtual-heart technology for guiding the ablation of infarct-related ventricular tachycardia. Nature Biomedical Engineering, 2018. 2(10): p. 732-740.

[7] Bayer, J.D., et al., A novel rule-based algorithm for assigning myocardial fiber orientation to computational heart models. Annals of Biomedical Engineering, 2012. 40(10): p. 2243-2254.

[8] Roca-Luque, I., et al., Post-ablation cardiac magnetic resonance to assess ventricular tachycardia recurrence (pam-vt study). European Heart Journal - Cardiovascular Imaging, 2023. 25(2): p. 188-198.

[9] Bayer, J.D., et al., The purkinje network plays a major role in low-energy ventricular defibrillation. Computers in Biology and Medicine, 2022. 141: p. 105133.

[10] Hillestad, M.L., et al., Myl4 identifies intramural anatomy of purkinje fibers in human hearts. JACC: Clinical Electrophysiology, 2025.

[11] Donahue, J.K., J. Chrispin, and O.A. Ajijola, Mechanism of ventricular tachycardia occurring in chronic myocardial infarction scar. Circulation Research, 2024. 134(3): p. 328-342.

[12] Arevalo, H.J., et al., Arrhythmia risk stratification of patients after myocardial infarction using personalized heart models. Nature Communications, 2016. 7(1): p. 11437.

[13] Trovato, C., et al., Human purkinje in silico model enables mechanistic investigations into automaticity and pro-arrhythmic abnormalities. Journal of Molecular and Cellular Cardiology, 2020. 142: p. 24-38.

[14] Yao, J.-A., et al., Remodeling of gap junctional channel function in epicardial border zone of healing canine infarcts. Circulation Research, 2003. 92(4): p. 437-443.

[15] Villar-Valero, J., et al., Computational modeling of post-myocardial infarction arrhythmias: Insights and predictions. Computers in Biology and Medicine, 2025. 196: p. 110894.

[16] Bhagirath, P., et al., From bits to bedside: Entering the age of digital twins in cardiac electrophysiology. Europace: The European Journal of Pacing, Arrhythmias and Cardiac Electrophysiology, 2024. 26(12).

[17] Álvarez-Barrientos, F., et al., Probabilistic learning of the purkinje network from the electrocardiogram. Medical Image Analysis, 2025. 101: p. 103460.

Address for correspondence:

Fuyu Cheng

Queen Mary University of London, 327 Mile End Rd, Bethnal Green, London E1 4NS

f.cheng@qmul.ac.uk